Separation Science and Technology
Publication details, including instructions for authors and subscription information:
http://www.informaworld.com/smpp/title~content=t713708471

Proton NMR Study of Micelle Formation in Surfactant Mixtures

Kanji Tamamushi[a]; David J. Wilson[a]
[a] DEPARTMENT OF CHEMISTRY, VANDERBILT UNIVERSITY, NASHVILLE, TENNESSEE

To cite this Article Tamamushi, Kanji and Wilson, David J.(1988) 'Proton NMR Study of Micelle Formation in Surfactant Mixtures', Separation Science and Technology, 23: 1, 1 — 15
To link to this Article: DOI: 10.1080/01496398808057630
URL: http://dx.doi.org/10.1080/01496398808057630

SEPARATION SCIENCE AND TECHNOLOGY, 23(1-3), pp. 1-15, 1988

Proton NMR Study of Micelle Formation in Surfactant Mixtures

KANJI TAMAMUSHI and DAVID J. WILSON*

DEPARTMENT OF CHEMISTRY
VANDERBILT UNIVERSITY
NASHVILLE, TENNESSEE 37235

Abstract

Proton spin-lattice relaxation times (T_1's) of micellar solutions of the nonionic surfactant Triton X-100 (TX-100, an alkylbenzenepolyethoxy alcohol) and of mixed micellar systems of TX-100 and *n*-dodecanol, *n*-dodecylamine, dodecyltrimethylammonium chloride, or sodium dodecylsulfate were determined. The results indicate that the hydrocarbon chains of the second surfactant penetrate to the aromatic rings of the TX-100 molecules, but do not extend to the region occupied by the alkyl chains of the TX-100. Ionic cosurfactants appear to produce a general loosening of the micellar structure, presumably because of their mutual coulombic repulsion.

INTRODUCTION

The use of mixed surfactant systems in the flotation of ores and minerals is well established (*1*, *2*), but these have not been employed until quite recently in precipitate and adsorbing colloid flotation separations. We investigated the theory of adsorption of binary surfactant mixtures on solid surfaces (*3*, *4*), and, on the basis of these findings, have begun experimental work using mixed surfactants in precipitate and adsorbing colloid flotation procedures (*5*).

If one is to optimize the performance of these mixed surfactant systems, it is necessary to have as detailed knowledge as possible about the interactions between the two surfactants in solution and in adsorbed

*To whom correspondence should be addressed.

layers on solid surfaces. Mixed micelle formation and solubilization studies can provide a good deal of information about surfactant interactions in solution (*6*, *7*), and a number of techniques have been used for this. One of the more useful is nuclear magnetic resonance (*8–12*).

We have carried out studies of the adsorption isotherms of dodecylsulfate on $Al(OH)_3$ and $Fe(OH)_3$ (*13*) and of the proton ^{13}C-NMR spectra of dodecylsulfate and dodecylbenzenesulfonate adsorbed on $Al(OD)_3$ (*14*). We have also used proton and ^{13}C NMR to investigate dodecanoic acid labeled at the carboxyl carbon and solubilized in anionic, cationic, and nonionic surfactants (*15*). Viscosity measurements were used to study the formation of extended micellar structures in mixtures of Triton X-100 (an alkylphenylpolyethoxy alcohol) and a number of other amphiphiles (*16*).

Here we report on a proton NMR study of Triton X-100 [TX-100, $(CH_3)_3CCH_2C(CH_3)_2C_6H_4(OCH_2CH_2)_9OH$] micelles and of mixed micelles containing TX-100 and a second amphiphile, such as dodecanol, dodecyl amine, dodecylsulfate, or dodecyltrimethylammonium ion. The objective of the study was to gain information about the interactions between surfactant species in micellar structures with the hope that this could be useful in understanding the behavior of hemimicelles of mixed surfactants on flocs, precipitates, and minerals.

EXPERIMENTAL

Scintillation grade Triton X-100 (TX-100) and commercial samples of dodecanol, dodecyltrimethylammonium chloride (DTAC), and 2-(2-ethoxyethoxy)ethanol were obtained from Eastman Kodak. Sodium dodecylsulfate (SDS) of 99+% purity was purchased from Sigma Chemical; its critical micelle concentration was measured by conductivity titration and found to be approximately 8.32 m*M* at 25°C. Dodecylamine (98% purity), deuterium oxide (99.8 atom% D), and deuterium oxide (99.8 atom% D) containing 0.75% 3-(trimethylsilyl)-propionic-2,2,3,3-d_4 acid, sodium salt (TSP), were obtained from Aldrich. Manganous sulfate monohydrate was Fisher's Certified Grade.

The D_2O was sparged with nitrogen to remove dissolved oxygen. Dodecylamine, dodecanol, SDS, and DTAC were solubilized in TX-100 solutions in D_2O at the desired concentrations. The solutions were transferred to 5 mm NMR sample tubes, blanketed with nitrogen, and capped. The ^1H spectra were obtained on a JEOL FX-90Q pulse Fourier transform NMR spectrometer operating at 89.55 MHz and using an

internal deuterium field-frequency lock on solvent D_2O. In addition, a few spectra were run on a Bruker AM-400 spectrometer operating at 400 MHz. All spectra were run at room temperature. The proton chemical shifts were measured with respect to internal standard TSP. A (180°-τ-90°-FID) pulse sequence was used to measure the proton relaxation times by the inversion-recovery method (*17*). The relaxation times were calculated by a nonlinear least-squares fit to the equation

$$M_z = M_{z0}[1 - 2 \exp(-\tau/T_1)] \quad (1)$$

The duration of a 180° pulse was determined by plotting signal amplitude versus pulse length for a solution of acetone in D_2O; the pulse yielding zero signal amplitude is a 180° pulse. This pulse length was determined by a linear least-squares plot of the data in the linear region in the vicinity of the zero in the signal amplitude.

RESULTS

The proton spectra of TX-100 at 90 and 400 MHz and the assignments of the peaks are given in Figs. 1 and 2. The assignments of the lines are as indicated. Assignment of the aromatic protons is based on the published assignments of the aromatic protons of *p*-methyl anisole and *p*-ethyl anisole (*18*).

The proton chemical shifts of TX-100 solutions of various concentrations are given in Table 1. These concentrations are all well above the critical micelle concentration for TX-100, which is about 0.3 m*M* (*19*). Table 2 contains chemical shift data for mixed surfactant solutions containing 200 m*M* TX-100 and various concentrations of a second amphiphile [*n*-dodecyl amine, *n*-dodecanol, *n*-dodecyltrimethylammonium chloride (DTAC), and sodium *n*-dodecylsulfate (SDS)].

The dependence of the proton T_1's on TX-100 concentration in D_2O solution is shown in Fig. 3. We note that the data for the aromatic protons were usually rather poor, as the peak intensities were much lower than those of the other peaks. This was true for all of our work on TX-100, and we therefore shall not attempt to interpret the aromatic proton results. Also, as will be seen later, the relaxation measurements for the ethoxy protons were somewhat complex; we report here the relaxation time of the major component of this system, and discuss the complexities in more detail later.

In Fig. 4 are plotted the T_1's of the protons giving the major peaks in the spectrum of TX-100–dodecylamine mixtures. The TX-100 concentration

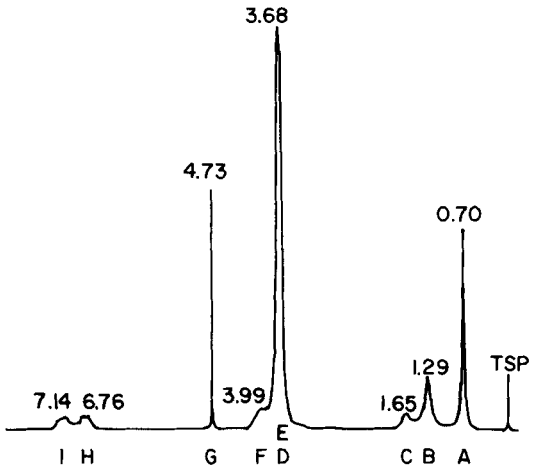

FIG. 1. The ^{1}H-NMR spectrum (90 MHz) of 200 m*M* TX-100 in D_2O at room temperature. Chemical shifts are given in ppm downfield from TSP. The peak assignments are as follows:

$((CH_3)_3CCH_2C(CH_3)_2-C_6H_4-OCH_2CH_2-OCH_2CH_2)_{8.5}$ OH/HDO

A C B I H F E D G

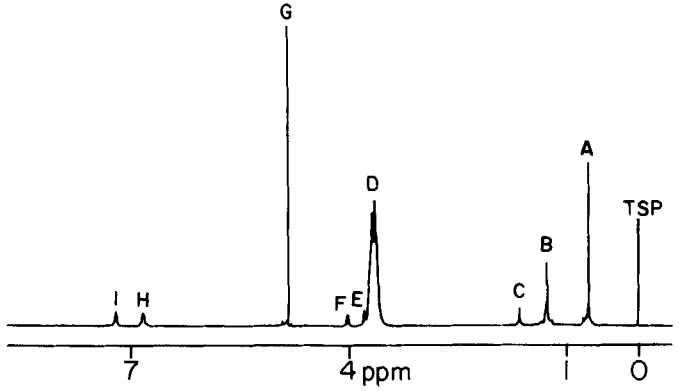

FIG. 2. The ^{1}H-NMR spectrum (400 MHz) of 100 m*M* TX-100 in D_2O. The peak assignments are indicated in Fig. 1. Chemical shifts are given in ppm downfield from TSP.

TABLE I
The Proton Chemical Shifts of TX-100

TX-100 (m*M*)	$(CH_3)_3-$ (ppm)	$(CH_3)_2-$ (ppm)	$-CH_2-$ (ppm)
In D_2O			
10.45	0.69	1.28	1.65
49.8	0.69	1.27	1.65
97.9	0.69	1.27	1.64
154.8	0.70	1.28	1.65
204.4	0.70	1.29	1.65
In 90% D_2O + 10% d_6-Acetone (by volume)			
10.0	0.70	1.28	1.67
50.0	0.70	1.28	1.65
100.0	0.70	1.28	1.65
200.0	0.71	1.30	1.67

was 200 m*M* and the dodecylamine concentration was varied over the range indicated.

The proton T_1's of solutions of TX-100 (200 m*M*) with concentrations of *n*-dodecanol ranging from 0 to 75 m*M* are plotted in Fig. 5. Proton T_1's of solutions containing 200 m*M* of TX-100 and varying concentrations (0 to 120 m*M*) of dodecyltrimethylammonium chloride (DTAC) are given in Fig. 6. The peak at 3.12 ppm is that of the *N*-methyl protons of the DTAC. Proton T_1's of solutions containing 200 m*M* of TX-100 and sodium dodecylsulfate (SDS) concentrations ranging from 0 to 110 m*M* are plotted in Fig. 7.

The proton T_1's of TX-100 at concentrations ranging from 10 to 200 m*M* in 90% D_2O–10% acetone-d_6 are shown in Fig. 8. The sensitivity of the spectrometer was not sufficient to allow the measurement of T_1's of TX-100 solutions in D_2O which were below the critical micelle concentration; addition of acetone should increase the cmc quite substantially, giving at least a qualitative picture of the behavior which one might expect from unmicellized TX-100.

T_1 measurements on 200 m*M* solutions of TX-100 with and without added Mn(II) (0.189 m*M*) are compared in Table 3.

TABLE 2
The Chemical Shifts of TX-100 Mixed Micelles

m*M*	$(CH_3)_3-$ (ppm)	$(CH_3)_2-$ (ppm)	$-CH_2-$ (ppm)	$-N(CH_3)_3^+$ (ppm)
Dodecylamine in TX-100 (200 mM)				
0.0	0.70	1.29	1.65	—
20.5	0.71	1.29	1.65	—
40.7	0.71	1.29	1.67	—
72.8	0.72	1.30	1.68	—
Dodecyl alcohol in TX-100 (200 mM)				
0.0	0.70	1.29	1.65	—
21.5	0.70	1.28	1.66	—
47.6	0.70	1.29	1.65	—
71.1	0.71	1.28	1.66	—
DTAC in TX-100 (200 mM)				
0.0	0.70	1.29	1.65	—
18.9	0.72	1.30	1.68	3.12
53.1	0.74	1.30	1.68	3.13
78.6	0.74	1.30	1.68	3.14
118.0	0.74	1.30	1.70	3.14
SDS in TX-100 (200 mM)				
0.0	0.70	1.29	1.65	—
17.3	0.70	1.29	1.65	—
40.2	0.70	1.28	1.67	—
69.4	0.70	1.29	1.67	—
104.0	0.71	1.30	1.68	—

CONCLUSIONS

From Tables 1 and 2 it is apparent that the proton chemical shift changes are too small to be of any use in characterizing these micelles. The chemical shifts remain virtually unchanged as the concentration of TX-100 is varied both in D_2O solution and in D_2O-acetone-d_6 solution. The critical micelle concentration of TX-100, 0.3 m*M*, is sufficiently low that it was not possible to make measurements on solutions of unmicellized TX-100. The quite major changes in micellar structure which result on the addition of dodecanol or dodecylamine, and which produce

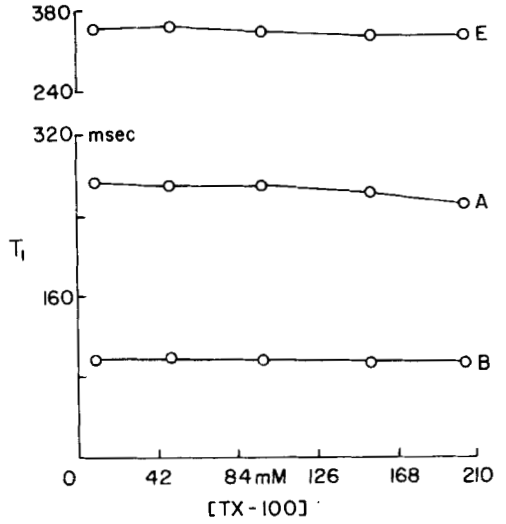

FIG. 3. Dependence of proton T_1's on TX-100 concentration in D_2O. The letters here and in the following figures refer to the labeling of the protons in Fig. 1. Note the break in scale at the ethoxy protons (E).

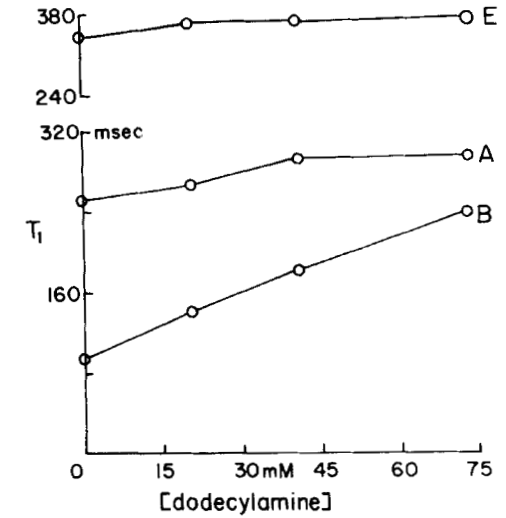

FIG. 4. Dependence of TX-100 proton T_1's on *n*-dodecylamine concentration in 200 m*M* TX-100 solutions in D_2O.

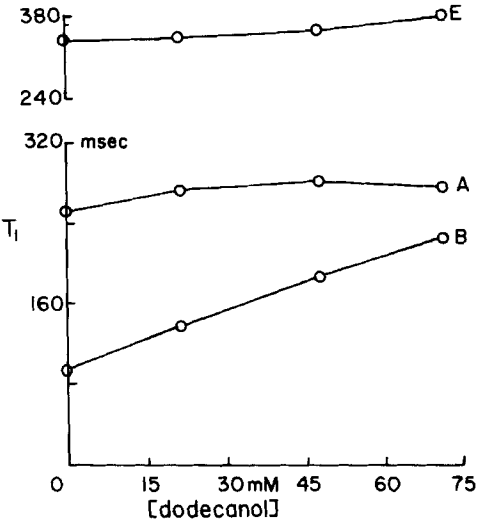

FIG. 5. Dependence of TX-100 proton T_1's on *n*-dodecanol concentration in 200 m*M* TX-100 solutions in D_2O.

very large increases in the viscosities of the solutions (*16*), produce negligible changes in the proton chemical shifts.

Increasing the TX-100 concentration does not seem to have any major effect on any of the proton relaxation times measured. See Fig. 3. All of the plots of T_1's show a slightly downward trend with increasing surfactant concentration, probably indicating minor micellar structure changes that decrease the freedom of motion of the protons as concentration increases.

The results shown in Fig. 4 indicate that the addition of *n*-dodecylamine to TX-100 results in relatively slight increases in the T_1's of all the protons except those in the methyl groups near the ring, which show a very marked increase in T_1. Mixed micelle formation appears to decrease the constraints on the protons in the branched alkyl chain, especially the protons in the methyl groups β to the benzene ring. Packing of the second surfactant into the micelle apparently is into the outer portion, decreasing the crowding on the alkyl chains in the micelle's core. The oxyethylene protons appear to be largely unaffected, suggesting that the dodecylamine molecules do not extend out much beyond the benzene rings of the TX-100.

The addition of *n*-dodecanol to TX-100 micelles produces results quite similar to those produced by the addition of dodecylamine, as seen by

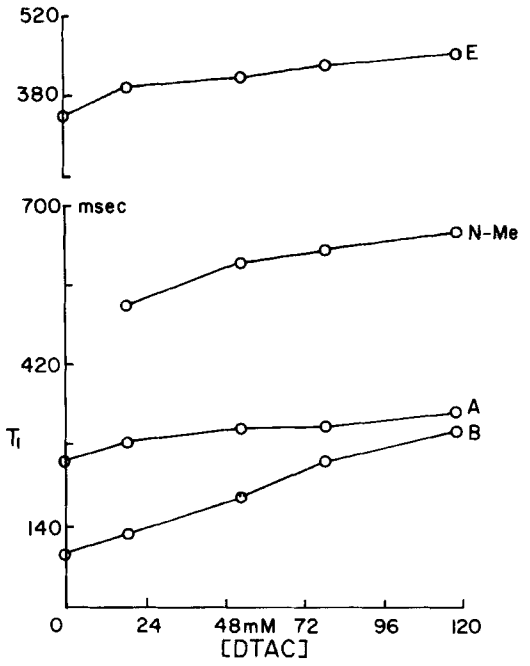

FIG. 6. Dependence of TX-100 proton T_1's on DTAC concentration in 200 mM TX-100 solutions. The DTAC N-methyl proton T_1's are also given.

comparing Figs. 4 and 5. Again, mixed micelle formation appears to decrease the constraints on the alkyl group in the micellar core, the protons in the methyl groups β to the ring being particularly affected. Evidently again the second surfactant is packing into the outer portion of the micelle, possibly increasing the crowding of the benzene protons (although our measurements on these are poor), and reducing the crowding of the alkyl group. Here, as with dodecylamine, the oxyethylene protons appear to be virtually unaffected, indicating that the dodecanol is not extending out very far into the hydrophilic portion of the micelle.

The relaxation times for protons in mixed micelles of TX-100 and dodecyltrimethylammonium chloride (DTAC) are shown in Fig. 6. The N-methyls of the DTAC were sufficiently intense and well-resolved so that their relaxation times were measured, in addition to those of the TX-100 protons. All of the T_1's increase with increasing DTAC concentration, including those of the N-methyls of DTAC, and also those of the oxyethylene groups of TX-100 (in contrast to what was observed with the

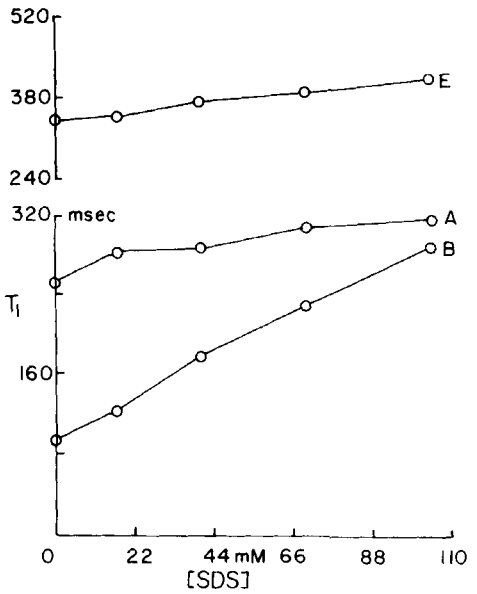

FIG. 7. Dependence of TX-100 proton T_1's on SDS concentration in 200 mM TX-100 solutions.

nonionic cosurfactants discussed above). Although the aromatic proton data are poor, they suggest that the constraints on even the hydrogens on the benzene rings are decreased as the DTAC concentration increases. Much the same effects were observed in mixed micelles of TX-100 and sodium dodecylsulfate (SDS), as seen in Fig. 7. In both cases this may be interpreted as indicating that the micellar structure is being loosened by the mutual coulombic repulsions of the ionic heads of these cosurfactants.

We note that the differences in relaxation times between mixed micelles containing nonionic cosurfactants and those containing ionic cosurfactants are not particularly large, despite the fact that viscosity measurements indicate major differences in overall micellar structure between these.

The T_1's of both the oxyethylene and alkyl groups are increased by the addition of acetone-d_6, as seen by comparing Fig. 8 with Fig. 3. This suggests that in the acetone-containing solutions the exchange rate of surfactant molecules into and from the micelles is increased and/or that the equilibrium is shifted somewhat toward the nonmicellized state.

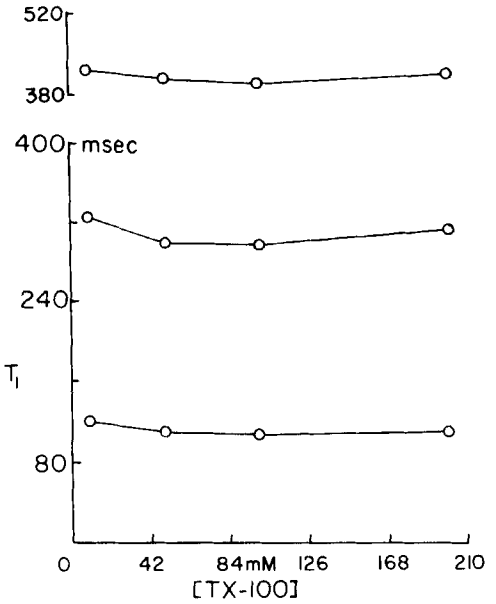

FIG. 8. Dependence of TX-100 proton T_1's on TX-100 concentration in 90% D_2O–10% acetone-d_6 (by volume).

Comparison of the T_1 data for TX-100 solutions with and without added Mn(II), given in Table 3, shows that the protons which are shielded from the aqueous solution by being buried in the hydrocarbon core of the micelle are much less affected by the presence of the paramagnetic ion. This suggests the use of such paramagnetic ions as

TABLE 3
T's of TX-100 with and without Paramagnetic Impurity

Chemical shift (ppm)	TX-100 only (200 mM) (ms)	TX-100 (200 mM) with Mn^{2+} ion (0.189 mM) (ms)	ΔT_1 (ms)
0.70	252.5	227.6	−24.9
1.29	95.2	90.0	−4.3
1.65	85.0	82.4	−2.6
3.68[a]	341.9	257.6	−84.3
3.74	587.5	460.9	−126.6
3.99	223.9	171.5	−52.4

[a]Main oxyethylene peak.

probes to determine the orientation of adsorbed surfactants as well as species in micelles.

Measurements of the T_1's of the oxyethylene protons yielding the peak at 3.68 indicated that apparently this is not a true single peak, but a multiplet of overlapping peaks with somewhat different relaxation times. The appearance of the oxyethylene resonance in (180°-τ-90°) experiments was therefore simulated for a number of values of τ, and the parameters in the model adjusted to determine if a satisfactory fit to the experimental line shapes could be obtained. The equations used to model the line shapes are as follows:

$$T_{1,i} = T_{1,0} + ai$$

$$\omega_i = \omega_0 + \beta i$$

$$i = 1, \ldots, N$$

$$S(\tau,\omega) = M_{z0} \sum_{i=1}^{N} \frac{1 - 2\exp(-\tau/T_{1,i})}{1 + ((\omega - \omega_i)/\Delta\omega)^2}$$

Here T_{1i} is the spin-lattice relaxation time for the ith oxyethylene group, ω_i is the Larmor frequency of the ith oxyethylene group, $\Delta\omega$ is the line width parameter used in calculating Lorentzian line shapes, τ is the time interval between the 180° and the 90° pulses, M_{z0} is the signal amplitude for a single 90° pulse, and $S(\tau,\omega)$ is the signal intensity. It was assumed that the chain contained 8 oxyethylene groups. For a 200-mM solution of TX-100, the best match between theory and experiment was obtained with the relaxation times and chemical shifts given in Table 4. Comparisons of calculated and observed NMR line shapes for the oxyethylene protons with these parameters are shown in Figs. 9 and 10, and appear to show reasonably good agreement. Rather poor measurements of the relaxation time of the protons at 3.99 ppm (shifted well downfield from the others by the ring current effect from the benzene ring) give relaxation times substantially lower than those found for the main oxyethylene peak. We therefore presume that the relaxation times of the oxyethylene protons increase as one moves out toward the OH end of the oxyethylene chain, in agreement with the expectation that the mobilities of the chain segments increase as one moves away from the bulky, rigid benzene ring.

Acknowledgment

This work was supported by a grant from the National Science Foundation.

TABLE 4
Parameters for Simulation of Oxyethylene Line Shapes Generated by (180°-τ-90°) Pulses

i	T_{1i} (s)	(Chemical shift)$_i$, ppm
1	.50	3.7500
2	.45	3.7214
3	.40	3.6928
4	.35	3.6642
5	.30	3.6356
6	.25	3.6070
7	.20	3.5784
8	.15	3.5498

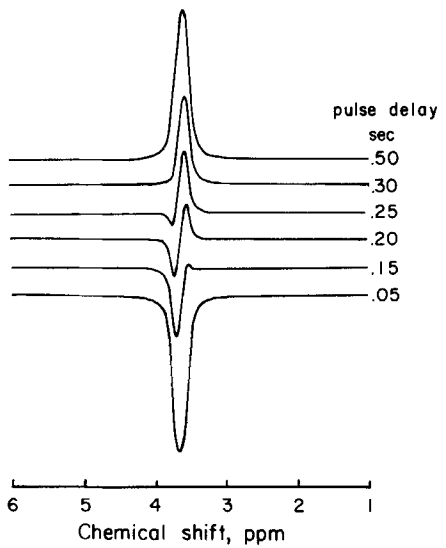

FIG. 9. Calculated line shapes for the major oxyethylene proton peak for various pulse delays. Parameters used in the calculation are given in the text.

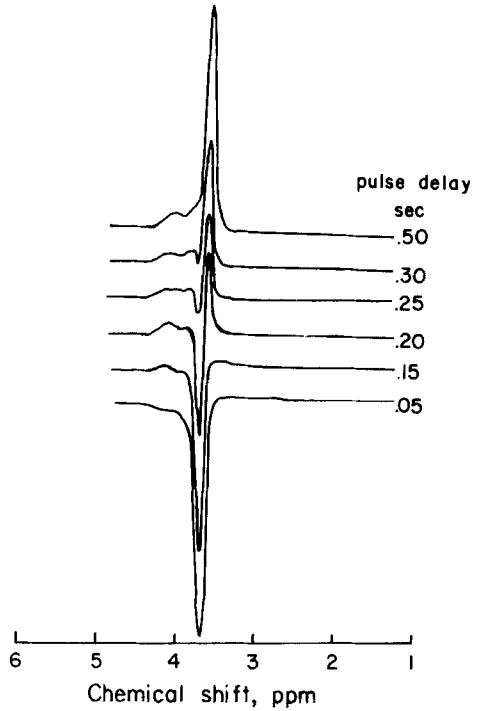

FIG. 10. Experimental line shapes for the major oxyethylene proton peak for various pulse delays. The sample is 200 m*M* TX-100 in D_2O, and the spectra were taken at 90 MHz.

REFERENCES

1. M. C. Fuerstenau (ed.), *Flotation—A. M. Gaudin Memorial Volume,* Vols. 1 and 2, American Institute of Mining, Metallurgical, and Petroleum Engineers, New York, 1976.
2. J. Leja, *Surface Chemistry of Froth Flotation,* Plenum, New York, 1982.
3. D. J. Wilson, *Sep. Sci. Technol., 17,* 1219 (1982).
4. D. J. Wilson and K. N. Carter Jr., *Ibid., 18,* 657 (1983).
5. M. Sarker, M. Bettler, and D. J. Wilson, *Ibid., 22,* 47 (1987).
6. B. Lindman and H. Wennerstrom, *Top. Curr. Chem., 87,* 1 (1980).
7. B. Lindman and H. Wennerstrom, in *Solution Chemistry of Surfactants: Theoretical and Applied Aspects* (E. J. Fendler and K. L. Mittal, eds.), Plenum, New York, 1982.
8. C. A. Bunton and M. J. Minch, *J. Phys. Chem., 78,* 1490 (1974).
9. J. Ulmius, B. Lindman, G. Lindbom, and T. Trakenberg, *J. Colloid Interface Sci., 65,* 88 (1978).
10. P. Stilbs and M. E. Moseley, *Chem. Scr., 15,* 175 (1980).
11. J. C. Eriksson, U. Henriksson, T. Klason and L. Odberg, in *Solution Behavior of Surfactants. Theoretical and Applied Aspects,* Vol. 2 (E. J. Fendler and K. L. Mittal, eds.), Plenum, New York, 1982, p. 907.

12. C. M. J. Chen and S. G. Frank, *J. Colloid Interface Sci., 92,* 399 (1983).
13. J. E. Kieffer, P. C. Sundareswaran, and D. J. Wilson, *Sep. Sci. Technol., 17,* 561 (1982).
14. W. Abraham, T. M. Harris, and D. J. Wilson, *Ibid., 19,* 389 (1984).
15. W. Abraham, T. M. Harris, and D. J. Wilson, *Ibid., 22,* 2269 (1987).
16. W. Abraham, K. Tamamushi, and D. J. Wilson, *Ibid., 22,* 1711 (1987).
17. R. J. Abraham and P. Loftus, *Proton and Carbon-13 NMR Spectroscopy,* Heyden, London, 1978.
18. W. W. Simons (ed.), *The Sadtler Handbook of Proton NMR Spectra,* Sadtler Research Laboratories, Philadelphia, 1978.
19. M. J. Rosen, *Surfactants and Interfacial Phenomena,* Wiley, New York, 1978.

Received by editor February 23, 1987